



Effect of cold reduction and annealing temperature on texture evolution of AISI 441 ferritic stainless steel

by M.G. Maruma*, C.W. Siyasiya†, and W.E. Stumpf‡

Synopsis

The effect of the amount of cold reduction and annealing temperature on the evolution of the texture of AISI 441 steel is reported. The steel was cold rolled by 62%, 78%, and 82%, followed by isothermal annealing of each sample at 900°C, 950°C, and 1025°C for 3 minutes. The crystallographic texture was determined by Phillips X'Pert PRO MPD texture diffractometer. Microstructures were characterized using optical microscopy and scanning electron microscopy (SEM). The results show that sample that received 78% cold reduction and annealing at 1025°C presented the highest R_m -value and lowest ΔR -value, which would enhance its deep-drawing capability. In addition, this sample showed the highest intensity of shifted γ -fibre, notably $\{554\}\langle 225 \rangle$ and $\{334\}\langle 483 \rangle$. It can therefore be concluded that the γ -fibre, which favours deep drawing, is optimal after 78% cold reduction and annealing at 1025°C.

Keywords

ferritic stainless steel, formability, texture, XRD.

Introduction

Global warming and air pollution are the major problems facing the world today. Therefore strict environmental legislation on the emission of harmful gases from motor vehicles has forced the automobile industry to search for alternative materials or new materials for exhaust systems. In order to produce cleaner exhaust gases, the exhaust temperature needs to be increased¹ to approximately 900°C. Exhaust manifolds are exposed repeatedly to hot gases as they are nearest to the engine, requiring good oxidation resistance, thermal fatigue properties, cold workability, and weldability. One such material to meet the above characteristics is AISI 441 ferritic stainless steel, a dual-stabilized Ti and Nb ferritic stainless steel. This 18%Cr stainless steel has good corrosion resistance at elevated temperatures. Ti and Nb are added to stainless steel to stabilize C and N due to their high tendency to form carbonitrides (Ti,Nb)(C,N) and laves phase² (Fe₂Nb) and Fe₃Nb₃C.

However, the drawability and stretchability of ferritic stainless steels is inferior to that of the more expensive austenitic stainless steels³. Furthermore, ferritic stainless steels also suffer

from undesirable surface defects known as ridging or roping. Therefore, considerable research has been carried out to understand the causes of ridging and roping in order to improve the steel's drawability⁴⁻⁶.

De Abreu *et al.*⁷ studied the effect of high-temperature annealing on texture and microstructure of an AISI 444 ferritic stainless steel. It was observed that samples cold rolled to 30% and 60% reductions and annealed at 1010°C presented the most suitable microstructure, texture, and R_m values for deep drawing. The main texture component found was $\{111\}\langle 112 \rangle$ and the texture contained no component in the $\{100\}$ plane. An increase in the annealing temperature from 955°C to 1010°C did not affect the grain size, but an increase in deformation decreased the grain size after annealing.

Huh and Engler⁸ studied the effect of intermediate annealing on texture, formability, and ridging of 17%Cr ferritic stainless steel sheet. It was found that intermediate annealing during cold working leads to a weak, but more desirable $\{111\} // ND$ γ -fibre texture with a lesser texture gradient. It has been shown that the formability of ferritic stainless steel can be improved by increasing the plastic strain ratio (R -value) which is related to the $\{111\}$ recrystallization texture⁷⁻¹⁰. The R -value in ferritic stainless steel can be improved by optimizing the chemical composition and processing

* Department of Materials Science and Metallurgical Engineering of the University of Pretoria, South Africa but now at Advanced Materials Division, Mintek, Randburg, South Africa.

† Department of Materials Science and Metallurgical Engineering of the University of Pretoria, South Africa.

© The Southern African Institute of Mining and Metallurgy, 2013. ISSN 2225-6253. This paper was first presented at the, Ferrous and Base Metals Development Network Conference 2012, 15-17 October 2012, Mount Grace Country House and Spa, Magaliesburg, South Africa..

Effect of cold reduction and annealing temperature on texture evolution of AISI 441

conditions, such as decreasing the carbon content, reducing the slab reheating temperature, increasing the annealing temperature, or refining the hot band grain size. The aim of this project is to optimize the process parameters at the industrial rolling mill, i.e. the annealing temperature and cold reduction.

Experimental details

Table I shows the chemical composition of the AISI 441 stainless steel, which was supplied by Columbus Stainless in a 4.5 mm thick hot band. The samples were cold rolled down to 62%, 78%, and 82% from the initial thickness in successive steps in a laboratory cold-rolling mill. The 62% cold-rolled specimen was used as a reference material, as this was equivalent to the industrially cold-rolled material. After cold rolling, the specimens were annealed at temperatures of 900°C, 950°C, and 1025°C for 180 seconds and then water quenched to freeze the microstructure.

The specimens were polished and then etched in a mixture of 100 ml H₂O, 100 ml HCl, and 100 ml HNO₃ for periods of between 30 and 90 seconds for microstructural analysis. For electron backscatter diffraction (EBSD), the specimens were electropolished in an alcohol solution of 5% perchloric acid using an applied voltage of 35 V DC for a period of 30 seconds. Microstructural analysis was carried out by both optical and scanning electron microscopy (SEM-EDS) on longitudinal sections of the rolling plane. The EBSD scans were performed in a FEI NOVA NanoSEM 230® FEG operated at 20 kV with LaB₆ filament. The bulk crystallographic texture that formed after each thermomechanical processing stage, namely cold roll and cold roll annealing, was measured by means of conventional X-ray texture analysis using a Phillips X'Pert PRO MPD texture diffractometer with a Cu K α radiation from three incomplete pole figures {110}, {200}, and {112} measured in back reflection. Orientation distribution functions (ODFs) were calculated by the series expansion method ($l_{\max} = 22$) using Mtex software,

which uses the MatLab platform. Orthotropic sample symmetry was applied and the orientations were expressed in Euler angles such that $0^\circ \leq (\phi_1, \theta, \phi_2) \leq 90^\circ$.

Tensile tests were used to assess the effect of annealing temperature on the formability of the sheet steel. The mean r -value (R_m) and planar anisotropy value (ΔR) were measured after 10% strain along the longitudinal, transverse, and diagonal directions. The R_m and ΔR -values were calculated using the following equations⁸:

$$R_m = \frac{r_{0^\circ} + 2r_{45^\circ} + r_{90^\circ}}{4} \quad [1]$$

$$\Delta R = \frac{r_{0^\circ} + r_{90^\circ} - 2r_{45^\circ}}{2} \quad [2]$$

where the subscripts 0°, 45°, and 90° refer to the longitudinal, diagonal, and transverse directions with respect to the rolling direction. The ΔR value represents the planar anisotropy of the materials and is the indication of the amount of necking or earing that will occur on the edges of the deep-drawn cups. The relationship between {111} intensity and R -value was examined for samples of thicknesses 1.5 mm, 1 mm, and 0.8 mm. In this study, the maximum orientation density of $\phi = 55 \pm 10^\circ$ in the $\phi_2 = 45^\circ$ section of the ODF was taken as representative of the {111} intensity [11].

Results and discussion

Microstructural analysis

Figure 1 shows the optical micrographs for cold-rolled samples after 62%, 78%, and 82% cold reduction. After cold rolling, the microstructure was composed of elongated ribbon-like grains with a large interior shear deformation. The grain boundaries arranged themselves parallel to the rolling direction with increasing strain, and the spacing between microbands tends to decrease with an increase in

Table I

Chemical composition of the type AISI 441 ferritic stainless steel (in mass %)

C	Cr	Mn	Co	V	Si	Ti	Nb	N	Ni
0.012	17.89	0.510	0.030	0.120	0.500	0.153	0.444	0.0085	0.19

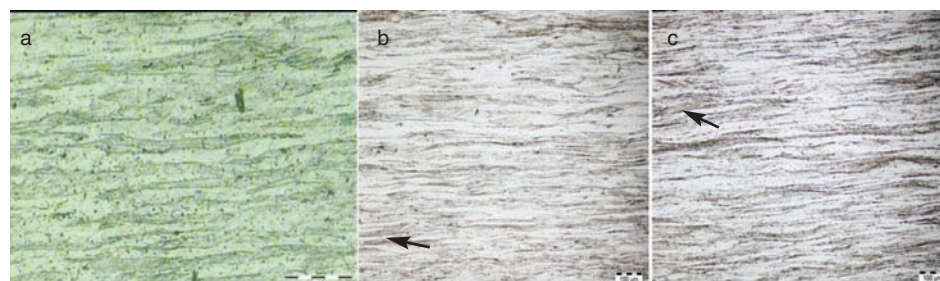


Figure 1—Effect of cold working on the microstructure of AISI 441 ferritic stainless steels; a, b, and c received 62% (typical of industrial cold work), 78%, and 82% cold work respectively

Effect of cold reduction and annealing temperature on texture evolution of AISI 441

strain. All three cold-rolled specimens show similar wavy fields that are strongly etched, while others are lightly etched, depending on the location on the microstructure. These are caused by deformation bands¹¹. Increasing the amount of cold reduction increases the non-uniform deformation regions (such as shear bands indicated by arrows) which act as nucleation sites for the {111} texture^{12,13}.

Figure 2 compares the grain sizes for the samples cold rolled to 62%, 78%, and 82% respectively and annealed at 1025°C for 180 seconds. The 62% cold-worked sample was produced with the typical industrial cold reduction. Contrary to expectation, the sample that was given the least cold reduction of 62% industrially resulted in the finest grain size. This suggests that the industrial cold reduction was somewhat not comparable to that of the laboratory. However, comparison of the two samples which were cold rolled using the lab mill show that increasing the cold reduction from 78%

to 82% led to further refinement of the grains due to higher driving force for static recrystallization.

As these ferritic stainless steels are stabilized with titanium and niobium, various kinds of precipitates such as TiC, TiN, Fe₂Nb, and Nb(C,N) are expected to form during different thermomechanical processing conditions¹⁴. Ti is a highly reactive element, which forms TiN precipitates at high temperatures in the melt in the presence of N, and forms TiC in the solid phase in the presence of C. Since Nb is a strong carbide former and has higher affinity for carbon than Ti, NbC will form preferentially to TiC during cooling, hence no TiC is detected by energy-dispersive X-ray analysis (EDX). Figure 3 shows the scanning electron micrograph with EDX analysis of a precipitate formed during hot band annealing of this AISI 441 steel. As may be seen, the Nb(C,N) precipitated heterogeneously on the rectangular TiN. This is due to the fact that TiN has a lower solubility in ferrite stainless steels

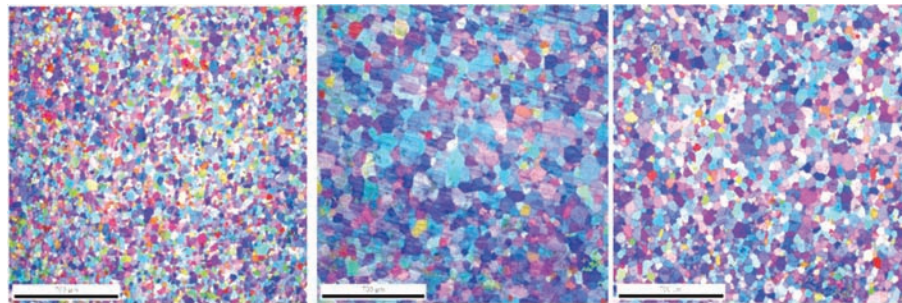


Figure 2—EBSD micrographs of AISI 441 ferritic stainless steels. a) 62% cold worked (industrially produced); b) 78% cold worked; c) 82% cold worked, showing grain size variations after cold work and annealing

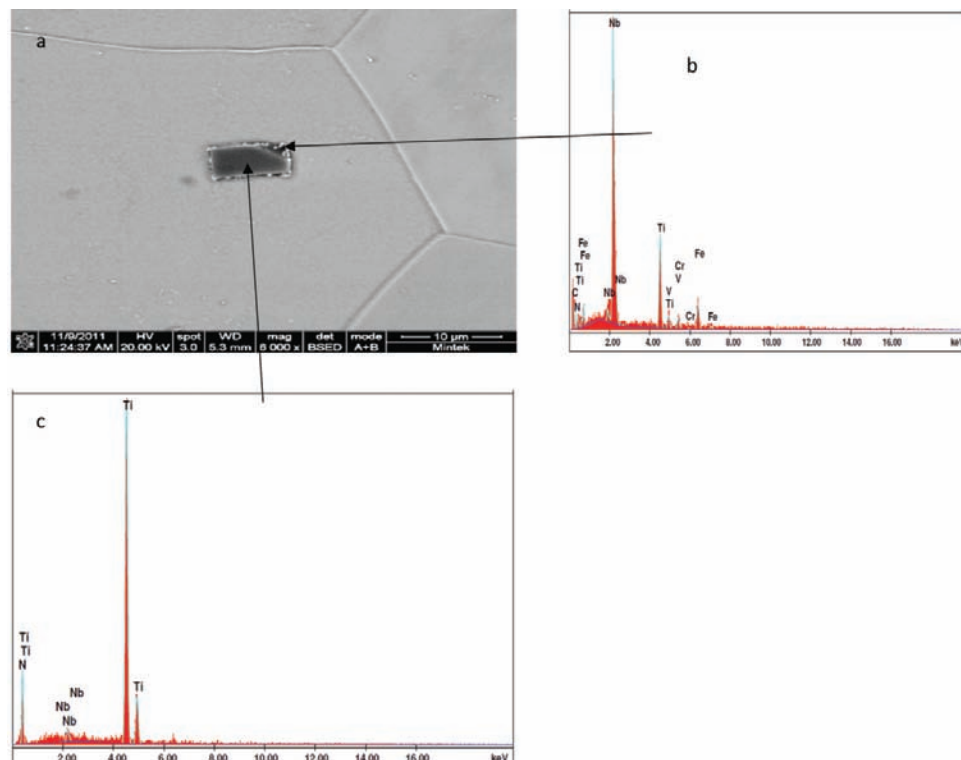


Figure 3—(a) SEM image and (b and c) SEM-EDX spectra of the as-received cold-rolled and annealed steel showing precipitate inside matrix

Effect of cold reduction and annealing temperature on texture evolution of AISI 441

than Nb(C,N) and will therefore form first during cooling from the melt³. Nb(C,N) forms at lower temperatures through heterogeneous nucleation on the existing TiN particle. This steel is interstitial-free when annealed at 1025°C as most of the carbon and nitrogen is tied by Ti and Nb.

Texture evolution

It is important to note that ferritic stainless steel (body-centred cubic or bcc) tends to develop or form a fibre texture during rolling and annealing. Rolling deformation in most cases leads to a texture characterized by two orientation fibres, i.e. an α -fibre texture comprising the orientation with a common $\langle 110 \rangle$ direction parallel to the rolling direction (RD// $\langle 110 \rangle$), while secondly, usually weak or less pronounced, is the γ -fibre comprising the orientation $\{111\}$ plane parallel to the rolling plane. Subsequent annealing of the cold-rolled sheets increases the γ -fibre at the expense of α -fibre¹³. All these orientations can be seen in a $\phi_2 = 45^\circ$ ODF shown in Figure 4.

Figure 5 shows the texture of the 62%, 78%, and 82% cold-rolled samples. The as-cold-rolled texture is characterized by strong α -fibre, notably $\{111\}\langle 110 \rangle$ and

$\{112\}\langle 110 \rangle$, orientation and weak γ -fibre. This is typical of cold-rolled bcc material⁷. The $\{111\}\langle 110 \rangle$ orientation increases with increasing amount of cold reduction.

Figure 6 shows the texture of the as-received cold-rolled sample, which is characterized by both γ -fibre i.e. $\{554\}\langle 225 \rangle$ and α -fibre $\{111\}\langle 110 \rangle$. A texture component in the $\{100\}$ plane, which has a negative influence on formability, is still retained even after annealing (Figure 6). Figure 7 shows the evolution of texture of the laboratory cold-rolled samples after annealing at different temperatures. Samples annealed at 900°C and cold-rolled with 78% and 82% deformation are characterized by a strong γ -fibre orientations with the maxima at $\{554\}\langle 225 \rangle$, $\{334\}\langle 483 \rangle$, and an α -fibre $\{111\}\langle 110 \rangle$.

As can be seen from Figure 7, α -fibre texture still prevails even after annealing at 900°C. This suggests that at 900°C, recovery is more dominant than recrystallization as recovery does not have much effect on the texture evolution. The intensity of α -fibre decreased prominently after recrystallization annealing at 1025°C. However, when the annealing temperature was increased to 1025°C, the γ -fibre was somewhat retarded and instead γ -fibre shifted to $\{334\}\langle 483 \rangle$

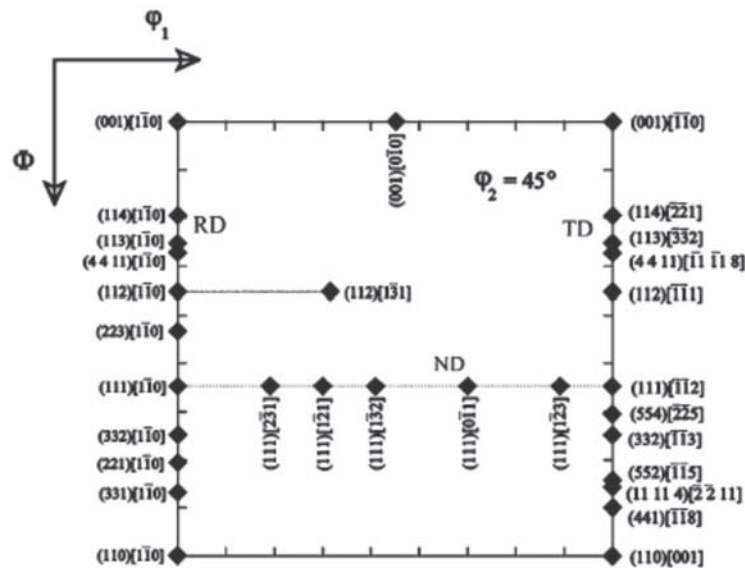


Figure 4— $\phi_2 = 45^\circ$ section showing the position of the main orientations in bcc steels along the RD, ND, and TD directions⁶

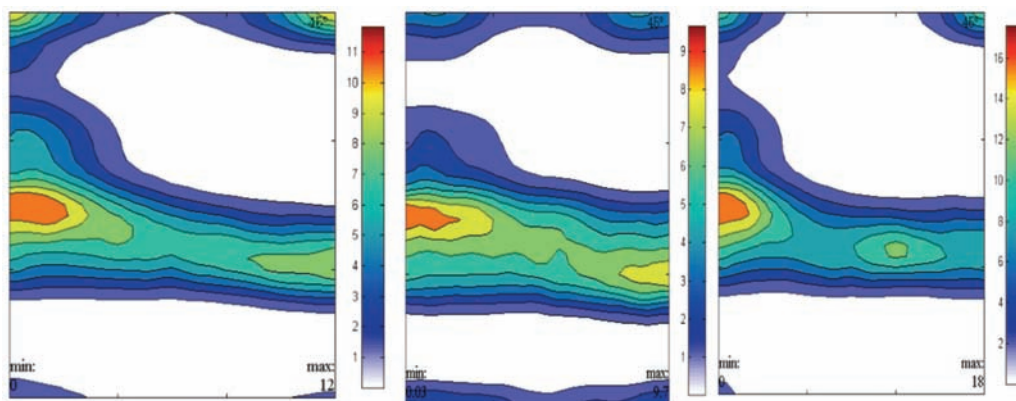


Figure 5—Bunge ODF $\phi_2 = 45^\circ$ for samples cold rolled to 62%, 78%, and 82%

Effect of cold reduction and annealing temperature on texture evolution of AISI 441

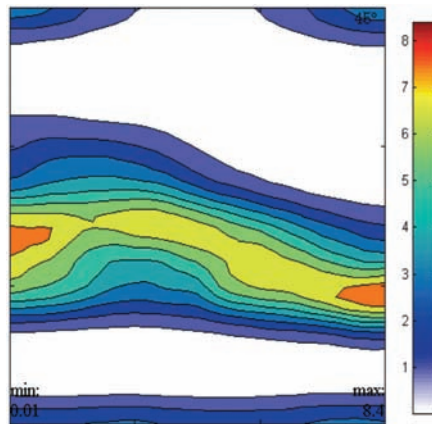


Figure 6—Bunge ODF $\phi_2 = 45^\circ$ for as-received hot band sample that was industrially cold-rolled 62% and annealed at 1025°C

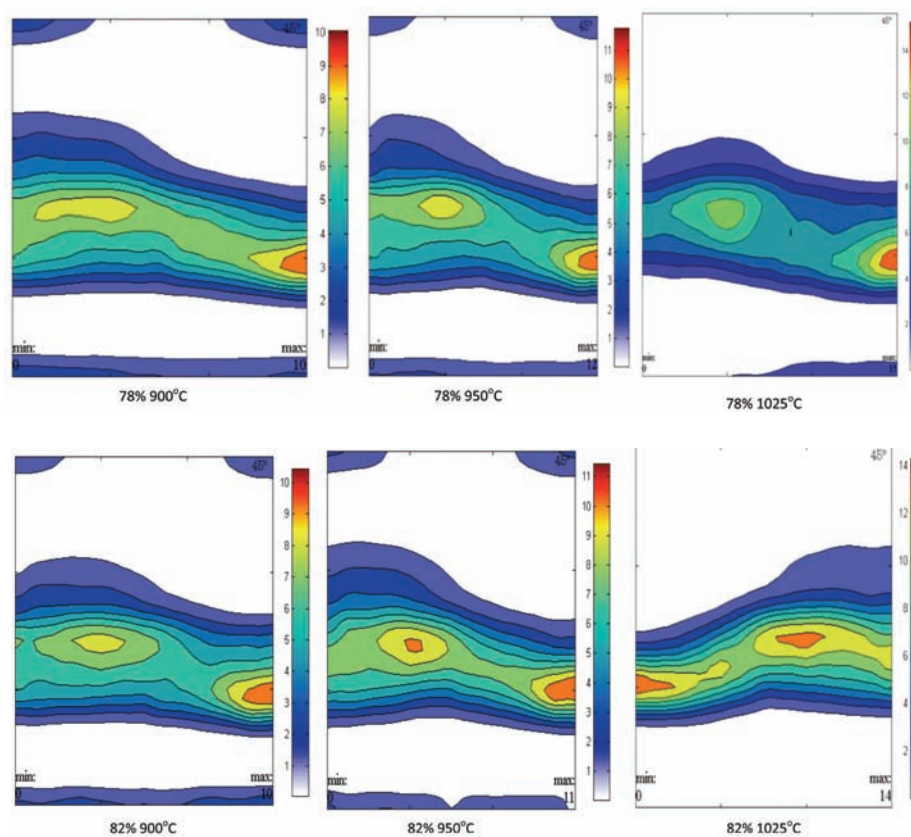


Figure 7—Bunge ODF $\phi_2 = 45^\circ$ for samples cold rolled 78% and 82%, each annealed at 900°C, 950°C, and 102°C

and $\{554\}\langle 225 \rangle$ in the 78% cold rolled samples. The $\{334\}\langle 483 \rangle$ is a texture which is shifted¹⁴ from $\{111\}\langle 112 \rangle$ by about 8° . Both $\{554\}\langle 225 \rangle$ and $\{334\}\langle 483 \rangle$ recrystallization texture and are related to the α -fibre $\{112\}\langle 110 \rangle$ by a $26^\circ\langle 110 \rangle$ which is close to a $27^\circ\langle 110 \rangle$ relationship having high mobility in bcc grain boundaries⁸. Therefore a selective growth mechanism plays an important role in the formation of these two annealing texture. It has been proposed by Raabe and Lucke that the retarding force of fine particles are responsible for a strong growth selection during recrystallization which leads to the growth of $\{334\}\langle 483 \rangle$ nuclei into the $\{112\}\langle 110 \rangle$ deformation matrix⁹⁻¹¹. This lead to the

strong formation of γ -fibre recrystallization texture with a strong shifts towards $\{334\}\langle 483 \rangle$ in ferritic stainless steels. Cold-rolled 82% and annealed samples show a strong shifted $\{110\}\langle 110 \rangle$ texture and moderate $\{111\}\langle 112 \rangle$. Both 78% and 82% cold-rolled samples that were annealed at 1025°C, shows no texture component in the $\{100\}$ plane. By and large, the γ -fibre is optimized when the steel is cold-rolled 78% and annealed for 180 seconds at 1025°C.

Effect of thermomechanical processing on formability

In order to assess the effect of the amount of cold reduction and annealing temperature on the formability of AISI 441

Effect of cold reduction and annealing temperature on texture evolution of AISI 441

Table II

Effect of Thermomechanical processing on Formability

Cold rolling	Annealing Temperature					
	900°C		950°C		1025°C	
	R_m	ΔR	R_m	ΔR	R_m	ΔR
62% CW (industrial)	-	-	-	-	1.37	0.4
78% CW	1.19	0.23	1.49	0.6	1.99	0.55
82% CW	-	-	1.3	0.49	1.7	0.5

ferritic stainless steel sheets, the R -values of the cold-rolled and annealed sheets were analysed. Calculated R_m - and ΔR -values for samples cold-rolled and annealed at three different temperatures are shown in Table II. The condition suitable for enhanced deep drawability as defined by the Lankford parameter is a high R_m -value and ΔR -values close to zero⁷.

The samples that were cold rolled by 78% and 82% and annealed at 1025°C exhibited the highest R_m -value, although their ΔR is higher than expected, with values far removed from zero. It is evident that the high R_m -values are associated with the strong γ -fibre $\{111\}$ //ND. The 78% and 82% cold-rolled samples annealed at 1025°C show higher intensity of $\{111\}$ orientations parallel to the normal direction compared to the 62% CW sample annealed at the same temperature. This observation is in agreement with Pickering and Lewis⁹, that high $\{111\}$ orientations are associated with high amounts of deformation, in excess of 75%. Increasing the amount of cold reduction increases the non-uniform deformation regions, which act as nucleation sites for $\{111\}$ texture¹¹. Samples cold rolled to 62% and annealed at 1025°C shows components in the $\{100\}$, which has negative influence on formability, hence lower R_m -value. The intensity of $\{554\}<225>$ is lower for the 62% cold-rolled sample compared to 78% and 82% cold-rolled samples after annealing. This clearly shows the important effect of cold reduction on formability.

As may be seen from Table II, no results were obtained from the samples that were given a cold reduction of 82% and annealed at 900°C, as they fracture before a tensile strain of 10%.

Conclusion

In this study, the effect of the amount of cold reduction and annealing temperature of AISI 441 ferritic stainless steel was examined. It can be concluded that the sample that received 78% cold reduction and annealing at 1025°C exhibited the highest intensity of shifted γ -fibre, notably $\{554\}<225>$ and $\{334\}<483>$. This is favourable for deep drawing.

Acknowledgements

The authors are grateful to Mr Richard Couperthwait (Engineer at Mintek) for helping with microtexture measurements and SEM examinations, and Mrs Grote from the Geology department at the University of Pretoria for XRD texture measurement. Warm appreciation must also go to Columbus Stainless for the provision of samples and to Mintek for further processing of the samples. The financial support from the Advanced Metals Initiative of the

Department of Science and Technology (AMI-DST) is very much appreciated. Permission to publish this work from both the University of Pretoria and Mintek is kindly acknowledged.

References

1. FUJITA, N., OHMURA, K., and YAMAMOTO, A. Changes of microstructures and high temperature properties during high temperature service of niobium added ferritic stainless steels. *Materials Science and Engineering A*, vol. A351, 2003. pp. 272–281.
2. SIM, G.M., AHN, J.C., HONG, S.C., LEE, K.J., and LEE, K.S. Effect of Nb precipitate coarsening on the high temperature strength in Nb containing ferritic stainless steels. *Materials Science and Engineering A*, vol. 396, 2005. pp. 159–165.
3. WEI, D., LAI-ZHU, J., QUAN-SHE, S., ZHEN-YU, L., and XIN, Z. Microstructure, texture, and formability of Nb+Ti stabilised high purity ferritic stainless steel. *Journal of Iron and Steel Research*, vol. 17, no. 6, 2010. pp. 47–52.
4. SHEPPARD, T. and RICHARDS, P. Roping phenomenon in ferritic stainless steel. *Materials Science and Technology*, vol. 2, 1986. pp. 693–699.
5. CHAO, H.C. Recent studies into the mechanism of ridging in ferritic stainless steels. *Metallurgical Transactions*, vol. 4, 1973. pp. 1183–1186.
6. TAKECHI, H., KATO, H., SUNAMI, T., and NAKAYAMA, T. The mechanism of ridging formation in 17% chromium stainless steel sheets. *Transactions of the Japan Institute of Metals*, vol. 8, 1967. pp. 233–239.
7. DE ABREU, H.F.G., BRUNO, A.D.S., TAVARES, S.S.M., SANTOS, R.P., and CARVALHO, S.S. Effect of high temperature annealing on texture and microstructure on an AISI 444 ferritic stainless steel. *Materials Characterization*, vol. 57, 2006. pp. 342–347.
8. HUH, M. and ENGLER, O. Effect of intermediate annealing on texture, formability and ridging of 17%Cr ferritic stainless steel. *Materials Science and Engineering A*, vol. 308, 2001. pp. 74–87.
9. RAABE, D. and LUCKE, K. Annealing textures of bcc metals. *Scripta Metallurgica*, vol. 27, 1992. pp. 1533–1538.
10. RAABE, D., HÖLSCHER, M., DUBKE, M., PFEIFER, H., HANKE, H., and LÜCKE, K. Texture development of strip cast ferritic stainless steels, *Steel Research*, vol. 64, 1993. pp. 359.
11. RAABE, D. and LUCKE, K. Influence of particles on recrystallisation textures of ferritic stainless steels, *Steel research*, vol. 63, no. 10, 1992. pp. 457–46.2
12. YAZAWA, Y., MURAKI, M., KATO, Y., and FURUKIMI, O. Effect of chromium content on relationship between r-value and $\{111\}$ recrystallization texture in ferritic steel. *ISIJ International*, vol. 43, no. 10, 2003. pp. 1647–1651.
13. ZHANG, C., LIU, Z., and WANG, G. Effects of hot rolled shear bands on formability and surface ridging of an ultra purified 21% Cr ferritic stainless steel. *Journal of Materials Processing Technology*, vol. 211, 2011. pp. 1051–1059.
14. YAN, H., BI, H., LI, X., and XU. Microstructure and texture of Nb+Ti stabilised ferritic stainless steel. *Materials Characterization*, vol. 59, 2008. pp. 1741–1746. ◆